ULUSLARARASI 3B YAZICI TEKNOLOJİLERİ
VE DİJİTAL ENDÜSTRİ DERGİSİ

INTERNATIONAL JOURNAL OF 3D PRINTING
TECHNOLOGIES AND DIGITAL INDUSTRY

ISSN:2602-3350 (Online)

URL: https://dergipark.org.tr/ij3dptdi

CHARACTERISATION OF 3D PRINTED HYDROXYAPITATE POWDER (HAp) FILLED POLYLACTIC ACID (PLA) COMPOSITES

Yazarlar (Authors): Hatice Kübra Yerli*, Kutay Çava, Mustafa Aslan

Bu makaleye şu şekilde atıfta bulunabilirsiniz (To cite to this article): *Yerli H.K.,* Çava *K., Aslan M., "Characterisation of 3D Printed Hydroxyapitate Powder (Hap) Filled Polylactic Acid (PLA) Composites" Int. J. of 3D Printing Tech. Dig. Ind., 6(3): 540-547, (2022).*

DOI: 10.46519/ij3dptdi.1172937

Araştırma Makale/ Research Article

Erişim Linki: (To link to this article): https://dergipark.org.tr/en/pub/ij3dptdi/archive

CHARACTERISATION OF 3D PRINTED HYDROXYAPITATE POWDER (HAp) FILLED POLYLACTIC ACID (PLA) COMPOSITES

Hatice Kübra Yerli[a]*, Kutay Çava[b], Mustafa Aslan[a,b]

[a] Metallurgical and Materials Engineering, Karadeniz Technical Universty, TURKİYE
[b] Medical Device Design and Manufacturing Research and Application Center, Karadeniz Technical Universty, TURKİYE

* *Corresponding Author: maslan@ktu.edu.tr*

(**Received:** 11.09.2022; **Revised:** 17.11.2022; **Accepted:** 28.12.2022)

ABSTRACT

Biomaterials are used in the treatment of advanced orthopedic diseases. Hydroxyapatite (HAp), a bio ceramic material, has an important place in the calcium phosphate family. Since HAp exhibits low mechanical properties, it is used together with polylactic acid (PLA), which has biodegradable properties. In this study, HAp was obtained by the combustion method and its morphological properties were analyzed by scanning electron microscope (SEM) and chemical analyzes by X-ray spectrometry. 3D mechanical test specimens were produced by Fused Deposition Melting (FDM) technique using Hap powder filled PLA filaments. Thermoplastic elastomer (TPE) was used to examine the effect of compatibilizer in PLA-HAp composite materials. Physical, thermal (thermogravemetric analysis, TGA), tensile and compression properties of PLA-HAp composite materials were investigated. Results indicated that TPE improved the interaction between between PLA and HAp powder. With the improved compability the regular distribution of HAp and the interfacial bond in PLA-HAp-TPE composite are better than the other test samples. When the mechanical properties are examined, the tensile and compressive strength values of PLA-HAp-TPE composites are 29.2% and 12.5% higher than those values of PLA-HAp composites, respectively. On the other hand, thermal stability of PLA-HAp-TPE composites composite showed higher thermal stability than those of PLA-HAp composites and gives lower percentage weight loss.

Keywords: PLA, HAp, Physical, Mechanical, Thermal Properties 3D Printed Samples.

1. INTRODUCTION

Biomaterials are used for bone regeneration. Biomaterials can be based on the areas that for metal, ceramic, polymer and others are used. Hydroxyapatite (HAp, ($Ca_{10}(PO_4)_6(OH)_2$)), β-tricalcium phosphate (TCP,$Ca_3(PO_4)_2$), which are the main phase of calcium phosphate in bone, and their derivatives and combinations are the most widely used ceramics for bone regeneration [1]. HAp is both a good bioactive material and has low solubility rates compared to other calcium-phosphorus (CaP) such as TCPs because of its high chemical stability [2]. Moreover, HAp exhibits desirable properties such as non-toxic, non-immunogenic, non-inflammatory, osteoconductive, and good osteointegration properties [3-4]. However, brittle and inherent stiffness of HAp means that it is difficult to convert it into the form required for bone replacement and implantations [5]. Also, the poor strength of HAp often limits its use for load bearing applications. To exploit the properties of HAp and overcome its associated limitations, HAp is combined with different polymers to produce suitable biomaterials [6]. Among these polymer materials, PLA, an aliphatic thermoplastic in semi-crystalline or amorphous structure, produced from sugar cane and starch, is widely used. Since PLA is biodegradable and biocompatible, it is used as an implant in the form of anchors, screws, plates, pins, rods [7].

In PLA-HAp composites, PLA improves the low mechanical properties of HAp, while HAp also increases the osteoconductive property of the implant when incorporated into PLA, and

HAp may also have the ability to neutralize acidic products degraded from PLA [8-9].

Talal et al. [10] stated that PLA-HAp composite materials have suitable mechanical properties for bone applications. The mechanical properties of PLA-HAp composites may vary according to the production methods. However, mechanical properties can increase by improving the interface between the filler (HAp) and the matrix (PLA) by including the compatibilizer material in the production of these composites. According to Akindoya et al. [7] investigated the effect of phosphate-based compatibilizer in improving the thermal and mechanical properties of PLA-HAp composites. They stated that the compatibilizer improved the thermal properties of HA composite materials. In addition, there was an increase of approximately 25%, 20% and 42% in the tensile, modulus and impact properties of the modified PLA-HAp composite, respectively. In another study, Cui et al. [11] prepared Nanohydroxyapatite (op-HAp), an oligomer (lac oligomer) grafted onto a surface-modified L-lactic acid oligomer, for bone repair. To examine the effect of grafting, 10% by weight of ungrafted HAp-PLGA and grafted HAp-PLGA has been compared. The cell porosity increased up to 90% in the grafted group. In addition, among the grafted HA/PLGA groups with 5% - 10% - 20% and 40% HAp additives by weight, 20% grafted HAp-PLGA with the best mechanical properties with flexural strength (4.14 MPa) and compressive strength (2.31 MPa) has given.

PLA and PLA-based biomaterials are easily processed by any of the methods such as extrusion, injection moulding, film casting, fiber spinning, stretch blow moulding, thermoforming, electrospinning, foaming and so on [7].

Recently, injection and extruder are widely used in the production of PLA-HAp added composite materials. Among the types of extruders, the twin screw extruder is a production method that is difficult to process [12] and suitable for combining additive and matrix materials. The raw material produced in the extruder device is used to create materials by using the FDM method, which is one of the additive production methods. Additive manufacturing has significant potential in medical applications due to its high flexibility [13].

In the creation of HAp-PLA composite materials, Fused Deposition Modeling (FDM), which is one of the 3D technology methods, is widely used. FDM is an attractive method for fabricating bone skeletons with controllable interior/exterior architecture due to its high flexibility in material handling, processing as well as high mechanical properties [14]. For this reason, FDM has become an elite manufacturing method routinely used to fabricate medical polymer-based implants [15]. Wu et al [16] produced a HAp-PLA composite synthetic trabecular model using the FDM method. They examined the mechanical and morphological properties of these models. According to the obtained results, they stated that the mechanical properties of 3D printed models were very close to those of human bone. They also stated that the FDM method is a great advantage for the creation of complex structures and high surface quality.

In this study, it was aimed to develop composite filaments using hyadroxyapatite powder and PLA polymer. In this way, the effect of the addition of HAp powder and TPE (thermoplastic polyester elastomer) as a compatibilizer to PLA polymer on the mechanical, thermal and morphological properties of PLA composite test specimens printed with FDM technology was investigated.

2. MATERIAL AND METHOD

2.1. Materials

HAp powders produced from biowaste was used as additive material and Poly-lactic acid (PLA, Zhejiang Hisun) was used as polymer matrix material. Thermoplastic polyester elastomer (TPE, Sasa company) was used to provide the flexibility of the filaments as a compability agent.

2.1.1 Production and pulverization of HAp

Sodium hydroxide (NaOH-) solution was used to destroy fat, meat and bone membrane found in beef rib bones. Sodium hydroxide solution was prepared with sodium hydroxide 10% w/w in distilled water. Beef rib bones were kept in solution for 24 hours and then dried in an oven. It was then burned at 750 °C for 12 hours. The resulting HAp was ground in a ball mill process. Ball milling was carried out at a speed of 350

rpm for 45 minutes intermittently (for every 2 minutes one minute stop). the HAp and tungsten carbur balls with 10 mm diameter were set to same weight during ball milling process. After the HAp was pulverized, it was subjected to in the size of 40 μm sieve as a powder size.

2.2. Production of Filament and 3D Mechanical Test Samples

In the production of composite filaments, HAp and TPE were added to PLA polymer as 10% and 3% by weight, respectively. Single-screw extruder was used in the production of pure PLA filament and twin-screw extruder was used in the production of composite filament. Both types of extruders have five thermal zones, the temperature in the zones between 160 °C and 190 °C in the initial and final zones, and pure and composite filaments with an average diameter of 1.75 mm were produced.

Tensile and compression test methods were used to examine the mechanical properties. Test samples were produced with Tevo brand FDM type 3D printer. Tensile test specimens were printed as 100*10*5 mm and compression test specimens as 10*10*10 mm as a full dense and one direction. The average of eight data from the same sample group was evaluated for both test methods. The printing parameters were given at Table 1.

Table 1. Printing paramters of test samples.

Parameters	Value
Layer thickness	0.3 mm
Wall thickness	0.4 mm
Infill density	100 %
Raster orientation	90 °C
Nozzle temperature	210 °C
Bed temperature	60 °C
Infill speed	40 mm/s
Fan speed	100 %

2.3. Examination of Physical Properties

2.3.1. HAp grain size analysis

Grain size measurement of HAp powders was made in a Mastersizer device (Malvern 2000). In the powder size analysis, using the wet method, was carried out after HAp about 200 mg of wieght were added to the distilled water in a baker of 2000 ml.

2.3.2. Morphology analysis of HAp powder and 3D test specimens

Scanning electron microscope (SEM, Zeiss Evo LS 10) was used to examine its morphological properties. Morphological analyzes were carried out to compare HAp powders obtained by wet precipitation and thermal combustion, and to examine the fracture surfaces of 100% filled standard tensile test specimens after testing. Each test sample was dried in a vacuumed oven before analysis and then subjected to gold plating (Au) treatment to increase conductivity.

2.4. Chemical Properties of HaP Powder

X-ray diffraction analyzes are used both to compare the phase compositions of HAp powders produced by two different methods and to control the phase compositions that will occur in the composite structure. The phase compositions of the HAp powder used as an additive were compared. Also, the neat phase structure of PLA used as the matrix material was compared with PLA composites mixed with thermoplastic elastomer (TPE) and HaP powder. X-ray diffraction analyzes were performed in PANalytical X-Pert3 Powder model device under Cu Kα (1.54 Angstrom wavelength) X-light source was set to 2θ angle between 20°and 60° with the step size 0.02 and step duration 0.5 sec.

2.5. Investigation of Thermal Properties

Thermogravimetric analysis was performed to determine and compare the thermal stability of PLA and composite filaments. Since the results of thermogravimetric analysis will vary depending on parameters such as gas flow, heating rate, sample weight, sample particle size, samples were analyzed by keeping all parameters constant in order to make accurate analysis and comparison. Thermogravimetric analyzes (TGA, Perkin Elmer 4000) were performed to begin 20 °C and ended with 600 °C. The analyzes were carried out with a gas flow rate of 10 °C/min in a nitrogen gas environment.

In order to examine the effects of HAp powder and compatibilizer on glass transition temperature, differential scanning calorimetry (DSC) analysis was performed on samples taken from PLA, PLA-HAp and PLA-HAP-TPE filaments with constant weight. DSC analyzes were performed on a Hitachi 7020 model, Japan device. In the DSC analysis, the samples were kept at 250 °C heated at a rate of 10 °C / min in the range of 25 °C to 250 °C for 2 minutes, then they were cooled at a rate of 10

°C / min in the range of 250 °C to 25 °C. The analysis was carried out under protective N_2 gas atmosphere at a rate of 30 ml/min.

2.6. Mechanical Test Methods

Mechanical tests were carried out on an universal testing machine (MTS model 45) using a 10 kN load cell with a crosshead speed of 5mm/min. Tensile test specimens were performed according to ISO 527-4&5 Plastic Composites. Compression tests were carried out according to the ASTM D 695 Plastics Compressive (Crosshead) test method.

3. RESULTS and DISCUSSION

3.1. Examination of Physical Properties

Grain size change and surface area in HAp powders according to the milling process order are shown in Table 2. While the grain size was decreased from 106.74 µm to 0.57 µm between the first milling and the final milling, the surface area was increased from 0.31 m^2/g to 13.9 m^2/g between the first milling and the final milling.

Table 2. Powder size and surface area after HAp powder.

Grind	d(0.1) (µm)	d(0.5) (µm)	d(0.9) (µm)	Surface area (m^2/g)
1	10,28	106,74	266,5	0.31
2	0.83	19.61	143.81	2.01
2	0.51	21.36	85.08	3.42
4	0.17	0.57	35.52	13.9

The images obtained at different magnifications in scanning electron microscopy (SEM) of HAp powders obtained by thermal combustion method are given in Figure 1a. When examined, it is seen that the powders do not exhibit agglomeration partially and are distributed almost homogeneously on the surface. Figure 1b shows that the powders are partially agglomerated on the surface. In Figure 1c, the powder shape is more prominent and it is seen that the powders are hemispherical.

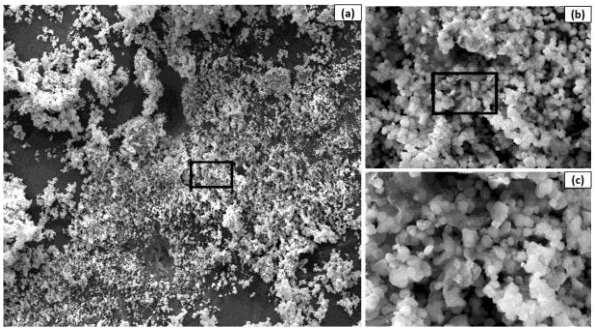

Figure 1. SEM (a) 500x, (b) 1000x and (c) 20000x magnifications of HAp powders.

After the tensile test applied to PLA and composite samples, SEM images were taken from the fracture surfaces of the samples. Bio-ceramic materials are brittle and have a porous structure for load bearing applications [17-18]. The bio-ceramic material hydroxypatite (HA) is a very brittle and porous material that exhibits brittle fracture. The fracture surface of neat PLA is shown in Figure 2a that surfaces shows ductile fracture patterns. PLA-HA composite materials, on the other hand, exhibit more ductile fracture than HA and more brittle fracture than PLA. Figure 2c shows the cross section of the composite sample consisting of PLA-HA combination. When this section was examined, it was observed that the fracture surface showed brittle fracture compared to the neat PLA. The effect of 3% TPE on the fracture surface can be seen in Figure 2d. Here, it is seen that the fracture surface of PLA-HAp-TPE is more ductile than the PLA-HAp fracture surface patterns.

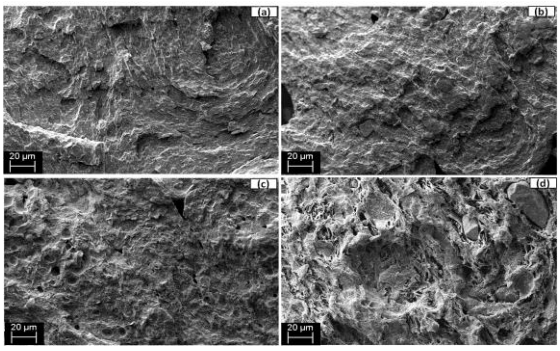

Figure 2. SEM images of fracture surfaces (a) PLA, (b) PLA-TPE, (c) PLA-HAp, (d) PLA-HAp-TPE.

3.2. Chemical Analysis of HAp Powders

In XRD phase analysis of beef bones kept at 750 °C for 12 hours, it was determined that they contained 99.6% HAp and it was observed that the obtained powders were semi-spherical.

When the literature was examined, Khoo et al. [19] worked at different temperatures in the thermal combustion method in their study and stated that organic-free natural HAp can be produced at temperatures of 700 °C and above. In XRD analysis, significant peaks of HA are located between the (002) and (300) planes between 25,900 and 32,920 [20]. As seen in Figure 3, the HA XRD analysis found (002), (211), (112), (300) planes at 25.9°, 31.9°, 32.30°, 33.03°, respectively.

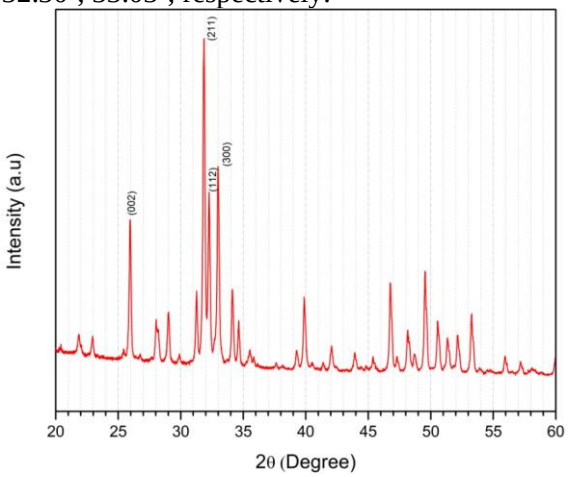

Figure 3. HA, XRD graph.

3.3. Thermal Preporties

TGA thermograms of PLA and composite materials were observed that the thermal decomposition temperatures between 30 °C and 600 °C in Figure 4. It is seen that the highest temperature belongs to PLA, that means that, its thermal decomposition resistance is higher than its composite form. When the percent weight loss of PLA and composites was examined, the highest loss was observed in PLA. The interfacial bonding force between the matrix and the additive material affects the thermal stability of the composite material. The active hydroxy (-OH) bonds in HAp strengthen the hydrogen (H) bonds with PLA [21]. Thus, the interfacial bond strength and thermal stability are increased.

The compatibilizing material (TPE) used in the composite structure may have regulated the distribution of HAp in the structure. With the new bonds formed and the regular distribution of HAp, the interfacial bonds in PLA-HAp-TPE samples are better thermal stability than the others. The thermal stability of PLA-HAp-TPE composites composite start to decrease thermal stability at higher temperatures than those of PLA-HAp composites and the lowest percent weight loss was seen in PLA-HAp-TPE.

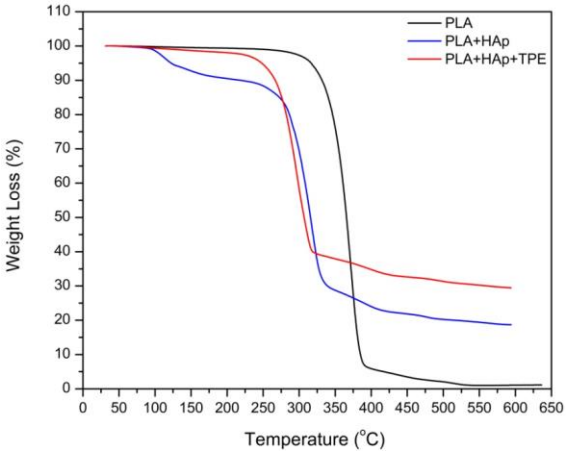

Figure 4. TGA thermogram graph of PLA and PLA-HAp composites.

When the heat flow-temperature graph of the DSC analysis applied to PLA and composite filaments between 25 °C and 250 °C is examined (Figure 5), the glass transition temperature (Tg) is observed, while the crystallization temperature (Tc) and melting temperature (Tm) are not seen. This is due to the amorphous structure of PLA, and it is observed that composites also exhibit amorphous behavior by being dependent on PLA. When the glass transition temperatures are examined, the Tg value of PLA is approximately 61 °C, while the Tg values of the composites are almost close to each other and vary between 55 °C and 60 °C. Commercial amourphous PLA was also characterised and confirmed typical DSC curve at similar Tg values [22].

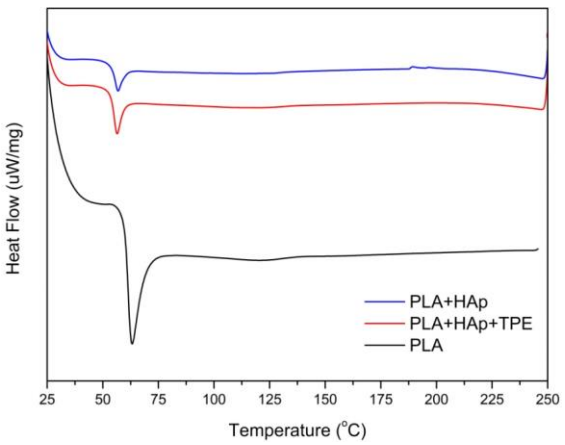

Figure 5. Heat Flow – Temperature of PLA and PLA-HAp composites.

3.3.1. Tensile Properties of 3D Printed Tension Test Specimen

Stress strain beheavior of 3D printed tensile specimens obtained from pure PLA and TPE and/or HAp mixed composite samples are presented the elongation of the samples during the test were presented. The highest strain to failure value was observed in the neat PLA sample as 5%. However, the PLA-HAp composite samples showed the lowest strain to failure with the value of 1.2%. On the other hand the addition of TPE to the composite shows the strain to failure value of 4.3% which is higher than the value of PLA-HAp specimens. While PLA-HAp-TPE showed more ductile faiure than those of PLA-HAp samples, (Figure 6) .

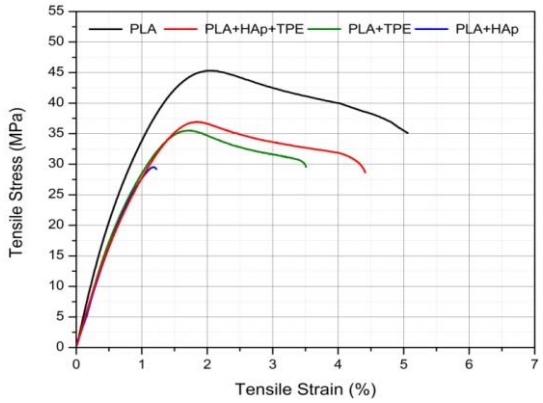

Figure 6. Tensile stress- strain behavior of 3D printed tensile test specimens.

In Figure 7, tensile strength and Young's modulus values of 3D printed test samples are presented. The results show that the highest average value was obtained at neat PLA samples (45 MPa) while the lowest average tensile stress was observed for PLA-HAp (27 MPa), with a decrease of 39% compared to the those of the neat PLA.

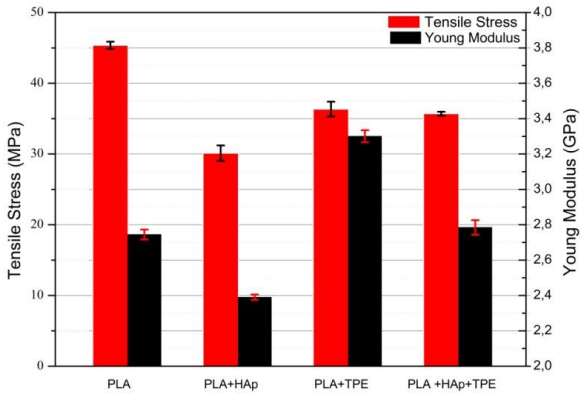

Figure 7. Tensile strength and Young modulus of 3D printed tensile test specimens.

When the effect of TPE on tensile strength of PLA composites was examined, a significant decrease of 27.4% was observed in values of PLA-TPE (35.3 MPa) composites compared to those of neat PLA sample. However, a significant increase of 29.2 % was observed in the values of PLA-HAp-TPE (35.8 MPa) composites with the addition of TPE compare to those of PLA-HAp composites.

Among the 3D printed tensile test specimens, the average values of Young's modulus from lowest to highest was obtained for PLA-HAp (2.4 GPa), PLA (2.6 GPa) , PLA-HAp-TPE (2.7 GPa), PLA-HAp (3.3 GPa) respectively (Figure 7).

3.3.2. Compression properties of 3D Printed Test Specimens

The typical compression stress and strain curves of pure PLA and TPE and/or HAp-mixed composite test samples are given in Figure 8. It is seen that all test speciments exhibit one distinctive behavior as a high slope in elastic region and then shows slow increase in nonlinear increase after highest stress point. The the compression strain at maximum stress was observed in PLA-HAp (0.12 mm/mm). on the other hand, PLA-TPE composite samples, showed the least strain value at max. stress (0.06 mm/mm). PLA-HAp-TPE (0.08mm/mm) composite samples showed 50% reduced compression strain compared to those of PLA-HAp samples.

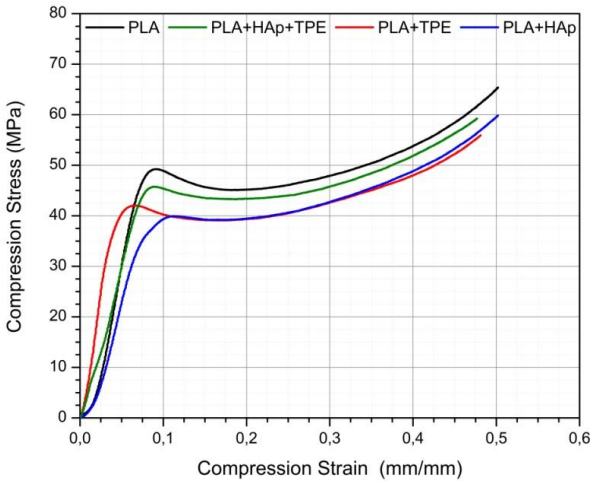

Figure 8. Compression stress- strain behavior of 3D printed compression test specimens.

In Figure 9, compression modulus and compression strength values of 3D printed test samples are presented. The highest average compression strength value belonged to PLA (47.8 MPa) samples. The lowest average compressive stress was observed in PLA+HAp (40 MPa), with a decrease of 19.5% compared to those of neat PLA. When the effect of TPE in composites was examined, a 16% decrease was observed in PLA-TPE (41.2 MPa) composites compared to those of neat PLA, while an increase of 12.5% was observed in PLA-HAp-TPE (45 MPa) composites compared to those of PLA+HAp composite.

Among the 3D printed compression test specimens, the average compression modulus from lowest to highest was PLA-TPE (0.9 GPa), PLA (1.1 GPa) , PLA-HAp-TPE (1.4 GPa), PLA-HAp (1.6 GPa) respectively (Figure 9).

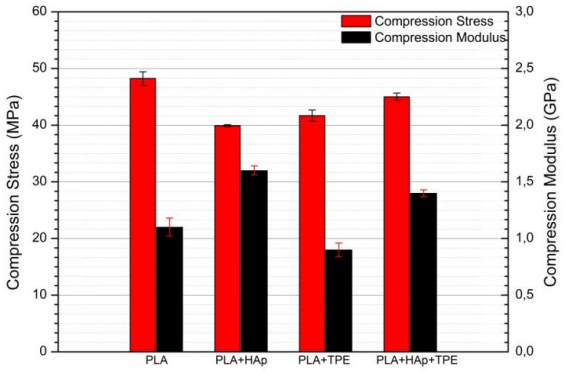

Figure 9. Compression strength and compression modulus of 3D printed compression test specimens.

4. CONCLUSION

HAp powders were obtained by thermal combustion method and 3D printed test samples were produced using FDM technique. In this study, it was investigated how 10% by weight HAp additive affects the mechanical, thermal and physical properties of PLA. Also, how TPE material changes the properties of PLA+HAp material is investigated. With the decrease of HAp grain size, the surface area increased in composite structures, which ensured that the powder distribution was homogeneous. When the test analyzes of the 3D printed tensile and compression test samples are examined, the tensile and compressive strength of PLA decreased with the HAp filler material. It has been observed that HAp decreases the strength of neat PLA while increasing the stiffness and brittleness of the structure of the neat PLA. It is also observed that TPE improves the mechanical, thermal and physical properties of PLA-HAP composite samples by increasing the surface interaction between HA and PLA in the structure.

ACKNOWLEDGES

This study was supported by the KTÜ-BAP 06 master's thesis project with the code FYL-2020-8621.

REFERENCES

1. Navarro, M., Michiardi, A., Castano, O., Planell, J.A., "Biomaterials in orthopaedics", J R Soc Interface, Vol. 5, Pages 1137–1158, 2008.

2. Takahashi, Y., Yamamoto, M., Tabata Y., "Osteogenic differentiation of mesenchymal stem cells in biodegradable sponges composed of gelatin and β-tricalcium phosphate", Biomaterials, Vol. 26, Issue 17, Pages 3587–3596, 2005.

3. Fu C., et al. "Antimicrobial silver-HAp composite coatings through two-stage electrochemical synthesis", Surf Coat Technol, Vol. 301, Pages 13–19, 2016.

4. Dorozhkin, SV., "Calcium orthophosphate deposits: preparation, properties and biomedical applications". Mater Sci. Eng. C., Vol. 55, Pages 272–326, 2015.

5. Akindoyo, J.O., Beg, M.D.H., Ghazali, S., Heim, H.P., Feldmann, M., "Effects of surface modification on dispersion, mechanical, thermal and dynamic mechanical properties of injection molded PLA-hydroxyapatite composites" Composites: Part A, Vol. 103, Pages 96-105, 2017.

6. Sun, F., Zhou, H., Lee, J., "Various preparation methods of highly porous hydroxyapatite/polymer nanoscale biocomposites for bone regeneration", Acta Biomater 2011, Vol. 7, Issue 11, Pages 3813–3828, 2011.

7. Auras, R., Lim, L.T., Selk, S.E.M., Tsuji, H. "Polylactic Acid, Synthesis, Structures, Properties, Processing and Applications", Wıley, NewYork, 2010.

8. Wang, T., Chow, L.C., Frukhtbeyn, S.A., Ting, A.H., Dong, Q., Yang, M., Mitchell, J.W., "Improve the strength of PLA-HA composite through the use of surface initiated polymerization and phosphonic acid coupling agent", Journal of Research of the National Institute of Standards and Technology, Vol. 116 Issue 5, Pages 785–796, 2011.

9. Reverchon, E., Pisanti, P., Cardea, S., "Nanostructured pllahydroxyapatite scaffolds

produced by a supercritical assisted technique", Industrial and Engineering Chemistry Research, Vol.48, Issue 11, Pages 5310-5316, 2009.

10. Talal, A., McKay, I., Tanner K., Hughes, F.J., "Effects of hydroxyapatite and PDGF concentrations on osteoblast growth in a nanohydroxyapatite-polylactic acid composite for guided tissue regeneration" Journal of Materials Science: Materials in Medicine, Vol. 24, Issue 9, Pages 2211-2221, 2013.

11. Cui, Y., Liu, Y., Cui, Y., Jing, X., Zhang, P., Chen, X., "The nanocomposite scaffold of polylactide-co-glycolide and hydroxyapatite surface-grafted with l-lactic acid oligomer for bone repair", Acta Biomaterialia, Vol. 5 Issıe 7, Pages 2680–2692, 2009.

12. Baird, D.G., "Polimer İşleme, Fiziksel Bilim ve Teknoloji Ansiklopedisi", Üçüncü Baskı, 2003.

13. Hoy, M.B., "3D printing: making things at the library", Med. Ref. Serv. Q., Vol. 32, Pages, 94–99, 2013.

14. Esposito, C.C., Gervaso, F., Scalera, F., Montagna, F., Maiullaro, T., Maffezzoli, S.A., "3D printing of hydroxyapatite polymer-based composites for bone tissue engineering", J. Polym. Eng. Vol. 37, Pages 741–746, 2017.

15. Youssef, A., Hollister, S.J., Dalton, P.D., "Additive manufacturing of polymer melts for implantable medical devices and scaffolds", Biofabrication, Vol. 9, Pages 1-29, 2017.

16. Wu, D., Spanou, A., Diez-Escuder, A., Persson, C., "3D-printed PLA HA composite structures as synthetic trabecular bone: A feasibility study using fused deposition modeling", Journal of the mechanical behavior of biomedical materials, Vol. 103, Issue 103608, Pages 1-10, 2020.

17. Rizzi, S.C., Heath, D., Coombes, A., Bock, N., Textor, M., Downes, S., "Biodegradable polymer hydroxyapatite composites: Surface analysis and initial attachment of human osteoblasts" J. Biomed. Mater. Res., Vol. 55, Pages 475 482, 2001.

18. Wang, H., Li, Y., Zuo, Y., Li J., Ma, S., Cheng, L., "Biocompatibility and osteogenesis of biomimetic nano-hydroxyapatite polyamide composite scaffolds for bone tissue engineering", Biomaterials, Vol. 28, Pages 3338–3348, 2007.

19. Khoo, W., Nor, F.M., Ardhyananta, H., Kurniawan, D., "Preparation of Natural Hydroxyapatite from Bovine Femur Bones Using Calcination at Various Temperatures" 2nd. International Materials Industrial and Manufacturing Engineering Conference, MIMEC2015, Procedia Manufacturing, Vol. 2, Pages 196 – 201, 2015.

20. Mahmud, K., Azharul Islam, M.D., Mitsionis, A., Albanis, T., Vaimakis, T., "Adsorption of direct yellow 27 from water by poorly crystalline hydroxyapatite prepared via precipitation method" Desalination and Water Treatment, Vol.41, Issue 1-3, Pages 170-178, 2012.

21. Yee, Y.Y., Ching, Y.C., Rozali, S., Hashim, N.A., Singh, R. "Preparation and characterization of poly (lactic acid)-based composites reinforced with poly dimethyl siloxane/ultrasound-treated oil palm empty fruit bunch" Polymer Technology Engineering, Vol. 54, Issue 13, Pages 1321–33, 2015.

22. Oguz, H., Dogan, C., Kara, D., Ozen, Z. T., Oavli, D. and Nofar, M., "Development of PLA-PBAT and PLA-PBSA bio-blends: Effects of processing type and PLA crystallinity on morphology and mechanical properties", A.I.P. Conference Proceedings 2055, 030003 January 2019.